Lab-on-a-Fish: Wireless, Miniaturized, Fully Integrated, Implantable Biotelemetric Tag for Real-Time *In Vivo* Monitoring of Aquatic Animals

Yang Yang, *Member, IEEE*, Jun Lu, *Member, IEEE*, Brett D. Pflugrath, Huidong Li, Jayson J. Martinez, Siddhartha Regmi, Bingbin Wu, Jie Xiao, and Zhiqun Daniel Deng

***Abstract*—*In vivo* electronic monitoring systems for underwater applications are promising technologies for obtaining information about aquatic animals. State-of-the-art devices are constrained by limits on the number of integrated sensors, large dimensions and weight, and short device longevity. Here, we report the Lab-on-a-Fish: the world's first biotelemetry tag that combines edge computing with wireless sensing of *in vivo* physiology [electrocardiogram (ECG) and electromyogram (EMG)], behavior [activity level and tail beat frequency (TBF)], and ambient environment (temperature, pressure, and magnetic field). The Lab-on-a-Fish has a miniaturized form (dry weight: 2.4 g; wet weight: 0.8 g; and dimensions: 5.5 mm × 6.5 mm × 37 mm) for studying small animals. Engineering efforts spanning improvements in battery chemistry, electronic circuit efficiency, and power-saving algorithms extend the longevity of the device to as much as eight months. The designed piezoelectric transducer and its driving circuit enable underwater wireless communication of multiplexed digital sensor data over a distance up to 400 m. The Lab-on-a-Fish can also store the raw data using flash memory for use in locations that are challenging for acoustic communications or when more complex data postprocessing is needed. Long-term *in vivo* validation in three species—rainbow trout (Oncorhynchus mykiss), white sturgeon (Acipenser transmontanus), and walleye (Sander vitreus)—demonstrated the device's sensing potential for biological and environmental applications.**

***Index Terms*—Biotelemetry, *in vivo* monitoring, integrated system, sensors.**

Manuscript received March 2, 2021; revised October 4, 2021; accepted November 1, 2021. Date of publication November 9, 2021; date of current version June 23, 2022. This work was supported by the U.S. Department of Energy (DOE) Water Power Technologies Office and Pacific Northwest National Laboratory LDRD Program. *(Corresponding author: Zhiqun Daniel Deng.)*

This work involved human subjects or animals in its research. Approval of all ethical and experimental procedures and protocols was granted by Pacific Northwest National Laboratory's Institutional Animal Care and Use Committee (protocol No. 2019-02) following the 8th Edition Guide for the Care and Use of Laboratory Animals (NRC 2011).

Yang Yang was with the Energy and Environment Directorate, Pacific Northwest National Laboratory, Richland, WA 99354 USA. He is now with the Institute of Deep-Sea Science and Engineering, Chinese Academy of Sciences, Sanya 572000, Hainan, China.

Jun Lu, Brett D. Pflugrath, Huidong Li, Jayson J. Martinez, Siddhartha Regmi, Bingbin Wu, and Jie Xiao are with the Pacific Northwest National Laboratory, Richland, WA 99354 USA.

Zhiqun Daniel Deng is with the Energy and Environment Directorate, Pacific Northwest National Laboratory, Richland, WA 99354 USA, and also with the Department of Mechanical Engineering, Virginia Tech, Blacksburg, VA 24061 USA (e-mail: zhiqun.deng@pnnl.gov).

This article has supplementary downloadable material available at https://doi.org/10.1109/JIOT.2021.3126614, provided by the authors.

Digital Object Identifier 10.1109/JIOT.2021.3126614

I. Introduction

AQUATIC biotelemetry technologies provide a means for inferences on locomotion, behavior, physiology, and ecology of tagged organisms in marine, freshwater, and estuarine ecosystems [1]–[3]. Through continuous monitoring of the biological processes and ambient environment of tagged animals, aquatic biotelemetry is accelerating our ability to predict the distribution and interactions of aquatic organisms across space and time, loss of biodiversity, and the disruption of ecosystem services resulting from anthropogenic and climate changes [4], [5]. Tagged animals can span sizes from the blue whale (*Balaenoptera musculus*) [6], Atlantic bluefin tuna (*Thunnus thynnus*) [7], and lemon shark (*Negaprion brevirostris*) [8] to significantly smaller ones, such as the American eel (*Anguilla rostrata*) [9], juvenile Pacific salmon (*Oncorhynchus spp.*) [10], and white sturgeon (*Acipenser transmontanus*) [11]. Accelerated prediction is essential to mitigating the changing global aquatic environment and steering its future management and conservation strategies [12]–[14].

Over the years, animal-borne biotelemetric devices (hereafter referred to as tags), which were initially used to simply track animals [6], [10], [15], have become equipped with sensors, including thermometers, barometers, accelerometers, magnetometers, gyroscopes, and physiological sensors [2], [16]–[19]. Nevertheless, state-of-the-art tags are still constrained to a limited number of sensors and peripherals integrated on an individual platform. For instance, to date, no commercial device can simultaneously monitor the electrocardiogram (ECG) and electromyogram (EMG), the two primarily studied physiological parameters of aquatic animals. No commercial device provides co-integrated physiology and behavior monitoring capabilities. A fully integrated, multifunctional tag would allow for correlating distinct physical, environmental, and physiological parameters of tagged animals to study the underlying biological processes. Tagged animals could also serve as mobile environmental sensing platforms in the Internet of Things [20], [21]. However, incorporating each additional functionality comes at the expense of the device's weight, size, and power consumption, posing challenges in circuit and software design, component optimization, and system integration. Another issue is that most existing sensor tags are large and bulky, causing a host to move unnaturally and become tired due to elevated energy expenditure [22]

and restricting the size and life stage of individuals that can be studied [23]. Although miniaturized tags [1], [3], [6], [10] have been demonstrated over the last decade, these devices have been limited to either tracking-only applications using an acoustic transmitter or integration with elementary sensors to satisfy size constraints. Furthermore, the lack of intelligent onboard data processing algorithms has hampered real-time examination of physiological and behavioral mechanisms. Consequently, current implementations are limited to storing data in onboard memory for offline diagnostics [6], [7], transmitting simple data (i.e., presence–absence flag or elementary sensor data) [2], [10], or continuously transmitting a large amount of raw data for real-time monitoring [24]. These approaches are not ideal, because they use a significant amount of onboard memory, require the animal to be recaptured (which is difficult) for data access, and drain batteries. In addition, the postprocessing algorithms on the receiver side may malfunction, even if only a small portion of the raw data fails to be received correctly [24]. Data processing at the signal edge [25] is highly desirable to extract the key physiological parameters from the continuous time-domain waveform for real-time sensor data transmission, and to reduce the onboard data storage use.

An ideal aquatic animal telemetry device would be a fully integrated platform, equipped with an arsenal of sensors and a high-capacity battery, coupled with efficient circuit and firmware design, flexibility in data acquisition, and intelligent onboard data processing, all while maintaining a small size and weight. Here, we introduce the Lab-on-a-Fish, a miniaturized, wireless, multifunctional, long life, fully implantable biotelemetry device, designed for continuous *in vivo* monitoring of aquatic animals. This is the world's first biotelemetric tag that can simultaneously measure ECG and EMG, as well as the physical behavior (acceleration and gyration) and ambient environment (temperature, pressure, and magnetic field) of the host. The Lab-on-a-Fish features a miniaturized form, weighing only 0.8 g in water and sized 5.5 mm $\times$ 6.5 mm $\times$ 37 mm, which is critically important for successful implantation in small animals. We utilized microbatteries small enough to create devices small enough for injection into an organism yet hold significantly more energy than similar-sized batteries. The developed tag features a flexible data acquisition approach: it can transmit the collected and onboard-processed data in real time entirely in digital format and store the raw data in onboard flash memory. Long-term *in vivo* evaluation was performed on 10 fish from three physiologically distinct fish species: rainbow trout (*Oncorhynchus mykiss*), white sturgeon (*Acipenser transmontanus*), and walleye (*Sander vitreus*). The evaluation demonstrated the Lab-on-a-Fish's capabilities in measuring aquatic animal behavior and physiology along with the ambient environment without interrupting natural daily activities.

II. Results

A. Design of the Lab-on-a-Fish

The objective of this study was to design and implement a device that can simultaneously monitor a tagged animal's physical, physiological, and ambient environmental parameters with a high signal-to-noise ratio (SNR); it also aimed to increase device longevity while maintaining a total volume and weight significantly lower than the state-of-the-art devices. These requirements mandate a compact, highly efficient device design, taking full advantage of recent advances in materials science, battery engineering, and integrated circuits (ICs) [26]–[30]. As shown by the 3-D rendering and photograph of the Lab-on-a-Fish [Fig. 1(a) and (b)], the key hardware components include the thin, multilayer printed circuit board (PCB), integrated sensors and peripherals, a piezoelectric transducer, and a microbattery. The device has been miniaturized: its dry weight is 2.4 g and its dimensions are 5.5 mm $\times$ 6.5 mm $\times$ 37 mm. The wet weight is only 0.8 g, which will substantially reduce the adverse effects of surgical implantation and tag burden on small animals.

The system consists of three functional modules [Fig. 1(c)]: 1) sensor module; 2) power management module; and 3) data transmission and storage module. The modular design makes the system customizable, upgradable, and reusable. The core of the system is a high-performance, low-power, 16-bit microcontroller unit (MCU) with a broad peripheral feature set. The sensor module contains off-the-shelf ICs and custom-designed circuitry employing analog front ends (AFEs) for monitoring the physiological (ECG and EMG) and behavioral [tail beat frequency (TBF) and activity level] characteristics of the tagged animal as well as the characteristics of the ambient environment (temperature, pressure, and magnetic field). The power management module enables a low-power operating system (8 μA during system sleep) by combining hardware and software optimization techniques. It exploits an in-house developed lithium metal/carbon monofluoride (Li/CF_x) microbattery with unprecedented battery performance [31], featuring a capacity of up to 60 mAh and a peak output current up to 50 mA, within a small package of 4.7 mm by 14.9 mm. An infrared (IR) sensor is used as the configuration interface using an IR "blaster" for efficient device programming and activation. The data transmission and storage module employs a rationally designed lead zirconate titanate (PZT) piezoelectric transducer and custom-designed driving circuitry for long-range (up to 400 m) underwater wireless communication. This module also holds an 8-MB nonvolatile flash memory with 20-year data retention to store raw sensor data for further advanced signal processing after the Lab-on-a-Fish is recovered.

A finite-state-machine model was adopted for the embedded software (firmware) implementation, which is responsible for performing all control, monitoring, data manipulation, and wireless communication functions. As illustrated in the simplified flowchart [Fig. 1(d), detailed in Methods], the firmware is always in one of the following four states: 1) initialization (*Init*) state for software and hardware configuration; 2) inactive (*Inactive*) state, in which the system is programmed in a low-power mode with all modules temporarily shut down; 3) active (*Active*) state for data acquisition, processing, and communication; and 4) download (*Download*) state for retrieving data from the onboard flash memory (Fig. S1 in the supplementary material). A hardware interrupt triggers the firmware to

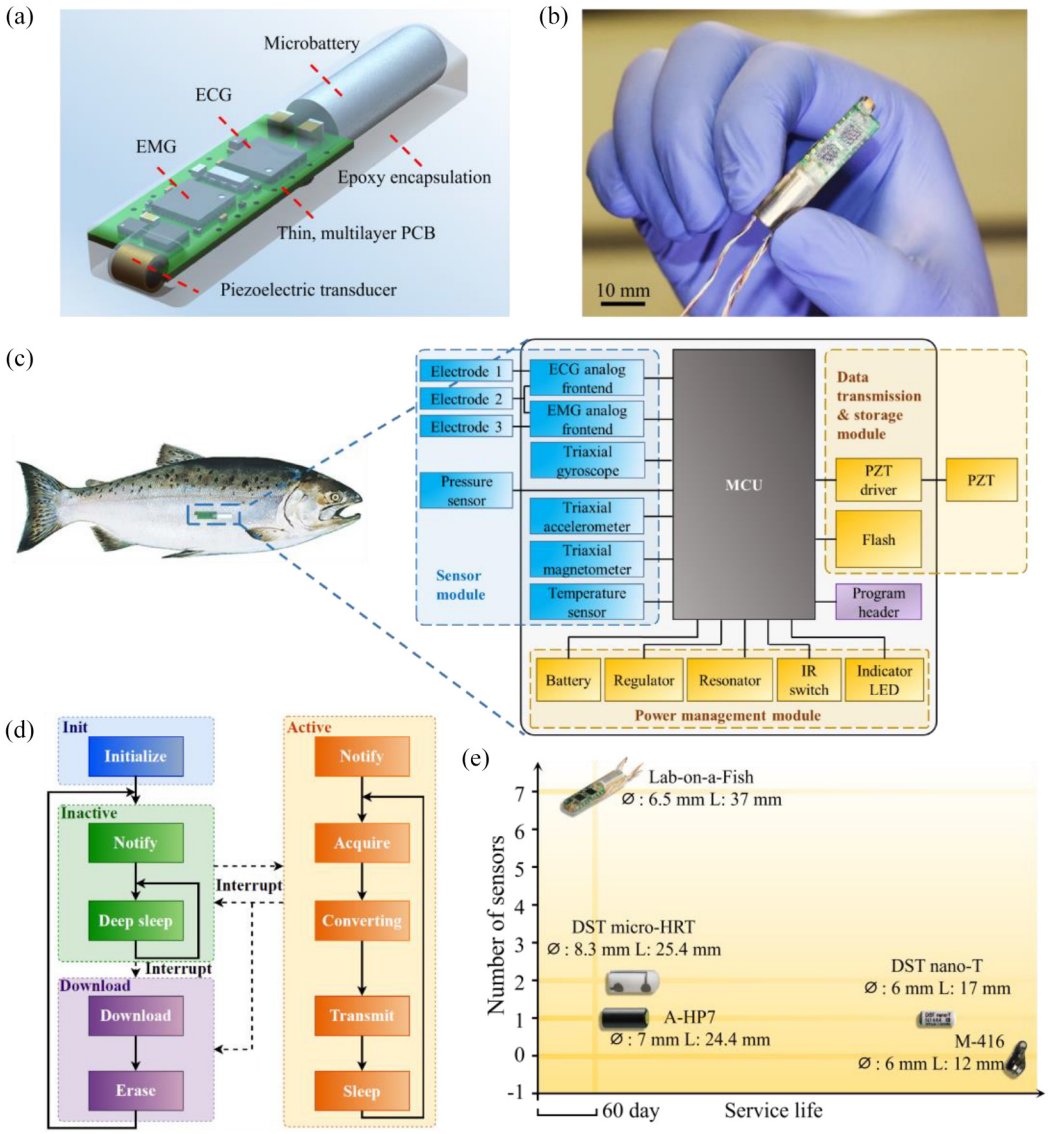

Fig. 1. Schematic illustrations and photograph of the Lab-on-a-Fish for wireless *in vivo* monitoring of aquatic animals' physiology, behavior, and ambient environment. (a) Three-dimensional (3-D) rendering of the Lab-on-a-Fish showing its key components, including the thin, multilayer PCB with sensors and peripherals, an acoustic transducer, and microbattery in biocompatible encapsulation. (b) Photograph of the device. (c) Hardware architecture of the Lab-on-a-Fish. (d) Simplified flowchart of the firmware. (e) Comparison with commercially available biotelemetric devices. The ratio of dimensions of different devices corresponds to their relative scale.

switch to a different state. The ability to hibernate (sleep) during the *Active* state for a user-specified length of time before beginning the next loop of data acquisition, processing, and transmission extends the device longevity.

The Lab-on-a-Fish has been compared with some representative commercially available devices considering their service life, number of sensors, and form factors, as illustrated in Fig. 1(e). The service lives of different devices are normalized to a data sampling interval of 10 min. The ratio of dimensions for different devices in the figure corresponds to their relative scale. Despite a service life up to 17 months, acoustic transmitter M-416 [32] does not include any sensor and can only send a presence–absence signal from the tagged animal. Similarly, even though a service life up to 14 months could be achieved by the DST nano-T [33], it could merely store simple temperature measurements without wireless communication capability. With more sophistication and each additional sensor, such as accelerometer and ECG, the device longevity declines exponentially with the design complexity. Our Lab-on-a-Fish outperforms the state-of-the-art commercial devices (DST micro-HRT [34], A-HP7 [35], M-416 [32], and DST nano-T [33]), providing an abundance of features while maintaining a comparable form factor and service life. The combination of these properties permits biologists and ecologists to apply a wider breadth of sensors to study smaller species for longer durations, which has not been possible with existing devices.

B. Manufacturing of the Lab-on-a-Fish

Manufacturing the Lab-on-a-Fish (Fig. 2) involves a combination of PCB manufacturing, component placement and soldering, thin-film deposition, and encapsulation. A series of small-footprint, high-performance, low-power operation, and

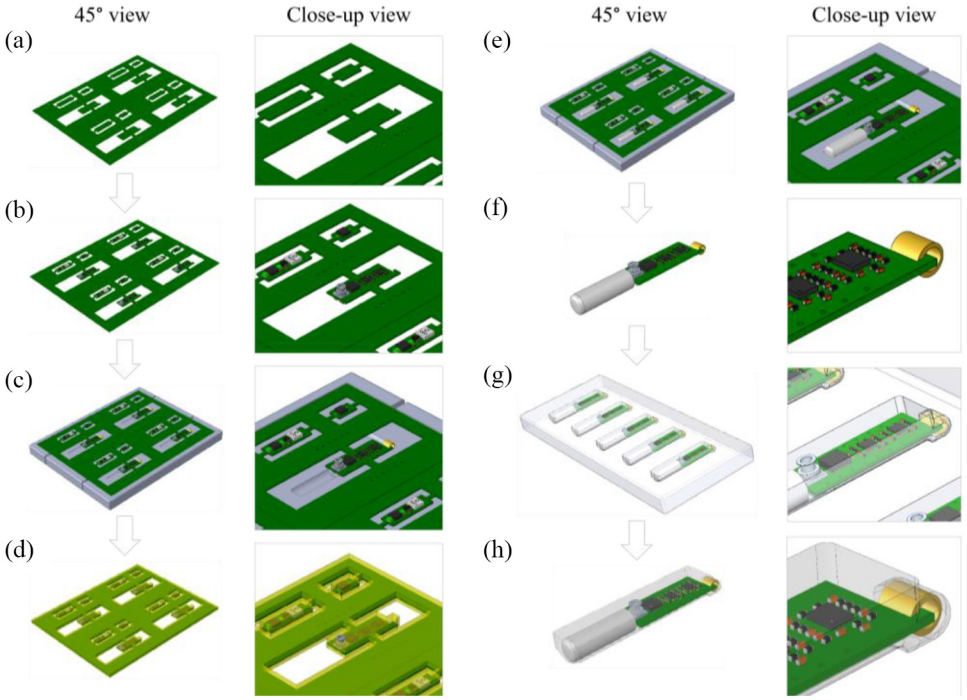

Fig. 2. Manufacturing process for the Lab-on-a-Fish with a 45° perspective and close-up view. (a) Manufacturing the thin multilayer PCB (four tags each). (b) Assembling the chips. (c) Attaching the PZT transducer. (d) Depositing a thin-film parylene-C layer. (e) Attaching the microbattery. (f) Cutting the main board off the panel. (g) Encapsulating the tag assembly using epoxy. (h) Attaching the ECG and EMG probes and applying the final parylene-C layer.

off-the-shelf electronic components forms the basis of the Lab-on-a-Fish. Our choice of commercially available electronics and manufacturing protocols supports the functional reproducibility of the devices and alignment with low-cost volume manufacturing, and permits further extension of functionalities of the platform with other sensors and peripherals for relevant monitoring applications [36]–[40]. The details of the manufacturing process are described in the methods.

C. Characterization of the Lab-on-a-Fish

1) Physiological, Behavioral, and Environmental Monitoring: The performance of the Lab-on-a-Fish's key functionalities and components was characterized individually, including multifunctional sensing, acoustic wireless communication, and microbattery.

The Lab-on-a-Fish can simultaneously monitor ECG and EMG with fully integrated biopotential measurement circuitry and onboard data processing algorithms. *In vivo* experimental validations were conducted initially on anesthetized rainbow trout (*Oncorhynchus mykiss*), white sturgeon (*Acipenser transmontanus*), and walleye (*Sander vitreus*), after which captive subjects swam freely in a tank. As shown in the schematic of the tagging protocol [Fig. 3(a), detailed in Fig. S2 in the supplementary material] and the photograph [Fig. 3(b)], surgical implantation of the Lab-on-a-Fish was accomplished with the ECG+ probe embedded subdermally into the tissue, just ventral of the pectoral fins, near the heart; the ECG−/EMG− and EMG+ probes were affixed subdermally near the lateral line, midway between the pectoral and pelvic fins; and the main tag was inserted into the body cavity. A biopotential acquisition circuit was designed [Fig. 3(c), detailed in methods] to extract, amplify, and filter small biopotential signals in the presence of noise. The circuit successfully monitored *in vivo* the physiological signals of all three species with a high SNR [Fig. 3(d), bottom row]. The voltage oscillations centered at half the peak voltage in the EMG signal [Fig. 3(d), top row] are associated with the axial musculature contraction. A clear QRS profile was visible from ECG measurements for all tested species. The QRS complex of the ECG signals is associated with the heart's functioning [41]. The measured heart rate (HR) variation correlates to a combination of parameters, including species, ambient environment, external stimulus, and history of behavior [Fig. 3(d)]. It is noteworthy that EMG artifacts can be present in the ECG from the swimming subject due that arise from muscle noise and probe motion, so a resilient data processing algorithm is needed.

An onboard, real-time ECG and EMG processing algorithm was implemented, allowing real-time transmission of the physiological data. The onboard ECG data processing algorithm, derived from Pan-Tompkins' real-time QRS detection algorithm [42], was designed and implemented to extract the HR from 6-s-long raw ECG waveform data. The 6-s data acquisition period was chosen to cover HRs down to 20 beats per minute (BPM). The ECG algorithm consists of a sequence of processing steps (Fig. S3 in the supplementary material) that include filtering, differentiation, amplitude squaring, moving-window integration, and discrimination of the QRS complex. Despite the limited amount of resources on the microcontroller, the implemented algorithms realized processing accuracy and low power consumption. The experiments on rainbow trout *in vivo* verified that the algorithm could detect the ECG peaks in real time with 99.4% accuracy

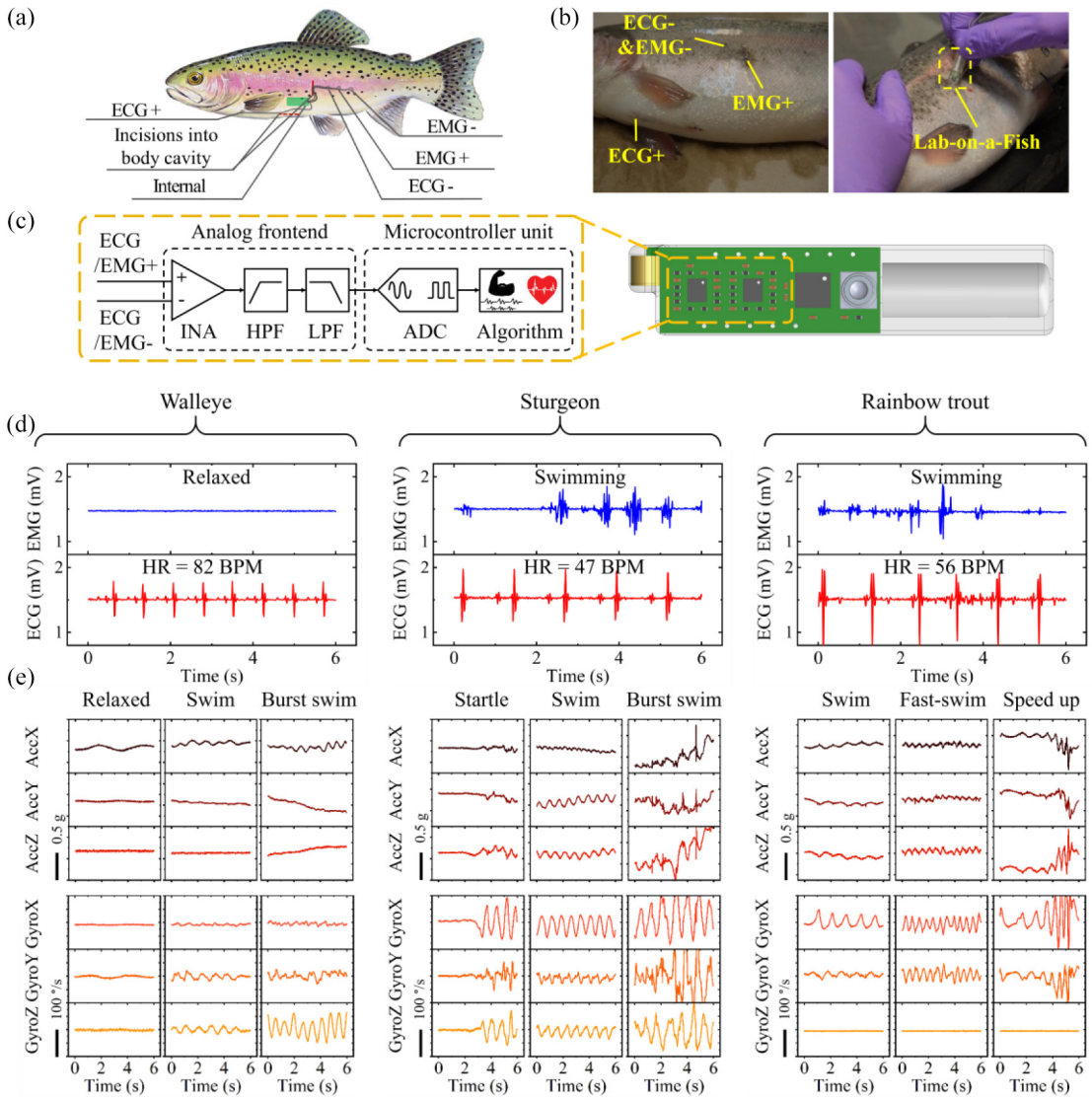

Fig. 3. Design and characterizations of the physiological and behavioral monitoring components. (a) Schematic illustration of the tagging protocol showing incision and probe locations, and Lab-on-a-Fish placement. (b) Photographs showing the surgical implantation procedure and the location of the Lab-on-a-Fish with the ECG and EMG probes. (c) Functional block diagram showing the ECG and EMG data acquisition and processing. HPF and LPF are high-pass and low-pass filters, respectively. (d) *In vivo* ECG and EMG signals, and (e) *in vivo* motion (triaxial gyration and triaxial acceleration) signals recorded in walleye, sturgeon, and rainbow trout swimming in a tank.

(Fig. S4 in the supplementary material). The onboard EMG data processing algorithm was designed and implemented to integrate a 6-s window of raw EMG waveform data with an index that represents the intensity of muscle activities.

The precise measurement of the behavior (e.g., activity level and tail beat activity) of aquatic animals in the field plays a key role in more accurately estimating their energy budget. The Lab-on-a-Fish incorporates small-footprint, off-the-shelf motion sensors, and onboard data processing algorithms for real-time behavioral monitoring. These motion sensors (triaxial gyroscope and triaxial accelerometer) record surging motion in the direction of the main axis of the animal (forward and backward), swaying motion along the axis crossing the animal body (side to side), and heaving motion on the vertical axis of the body (up and down). *In vivo* motion signals recorded in walleye, sturgeon, and rainbow trout [Fig. 3(e)] at 100 Hz show that different behavior patterns can be easily distinguished, including relaxing, startle, swimming, burst swimming, speeding up, and stopping. The behavior was confirmed by visual analysis of the recorded video. Data processing algorithms were applied to convert raw motion-sensor data to parameters that relate to fish behavior. The periodic patterns of the motion signals obtained from the dynamic behavior allowed fast Fourier transform (FFT) analysis to be applied (Fig. S5 in the supplementary material). The obtained spectrum enables assessment of the TBF of the tagged fish, which correlates to swimming speed [43]. Additionally, integration over the 6-s period along the trend line allows us to obtain the overall dynamic body activity. The X, Y, and Z components from the gyroscope were summed, and the resulting value is herein termed “activity level” (Act Lvl), with no specific units. The Lab-on-a-Fish also integrates temperature, pressure, and magnetic field sensors for real-time environmental monitoring. These sensors are critical for understanding the

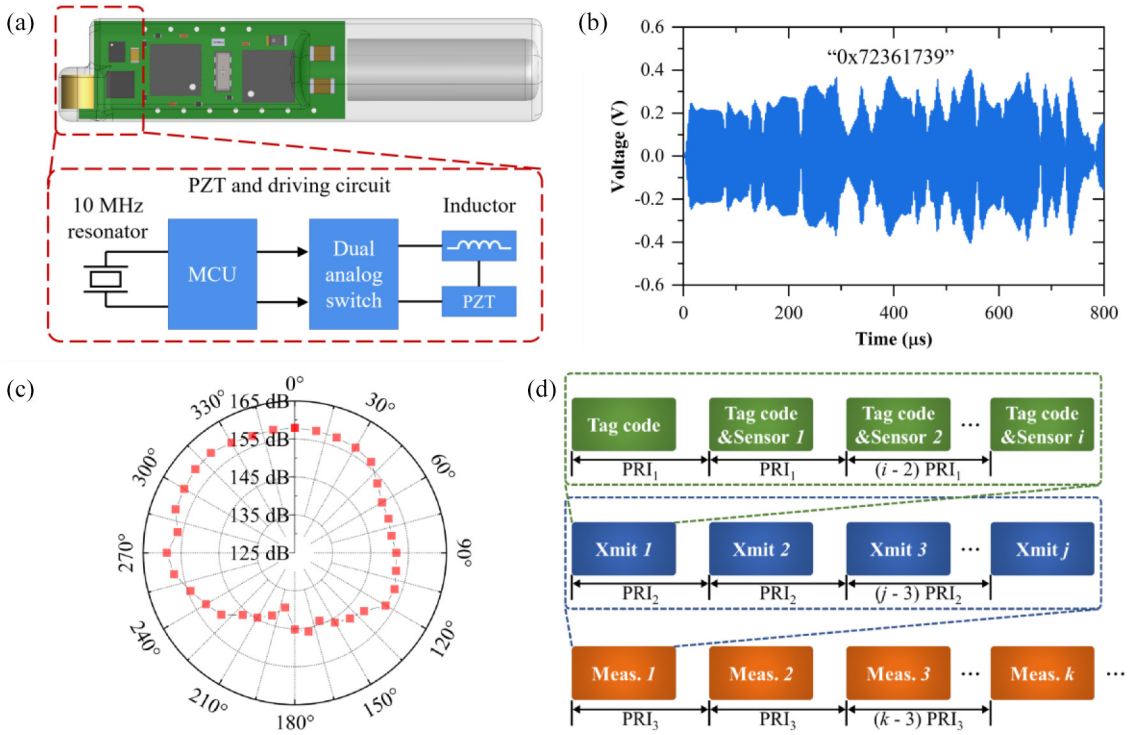

Fig. 4. Design and characterizations of the wireless acoustic communication. (a) Functional block diagram of acoustic wireless communication electronics. (b) Example of a transmitted acoustic wave with hexadecimal data "0x72361739," which includes the Barker code (0x72), the payload (0x3617), and the CRC code (0x39). (c) Polar plot of the acoustic signal radiation pattern. The source level is graphed as a function of the radiation angle. (d) Schematic illustration of the protocol for time-variant acoustic data communication, based on transmitting multiplexed unique digital identification (tag code) and sensor data, entirely in digital format. "Xmit" denotes transmissions. "Meas." denotes measurements.

behavior, providing additional insight on physiology, and serve as a potential future mobile environmental monitoring platform in the Internet of Things [20]. Characterizations of the environmental sensors are available in Fig. S6 in the supplementary material.

2) Design and Characterizations of the Wireless Acoustic Communication: The Lab-on-a-Fish employs acoustic waves—the most versatile and widely used physical layer technology for underwater wireless communication [44]. The acoustic communication module [Fig. 4(a)] consists of a ceramic-tube piezoelectric transducer and a custom-designed driving circuit. The dimensions and geometry of the transducer were designed to achieve a hoop-mode resonance frequency of 416.7 kHz, which is typically beyond the background noise in turbulent aquatic environments, and to achieve an omnidirectional acoustic beam pattern. During operation, the driving circuit emits a binary phase-shift keying (BPSK)-encoded waveform through an analog switch onto one side of the PZT, to generate time-critical signals at 416.7 kHz. A series inductor on the opposite side of the PZT establishes resonance with the transducer's fundamental capacitance. As a result, a much higher effective driving voltage of up to 15 V is achieved, producing a stronger signal and thus, a longer transmission distance. Fig. 4(b) shows an example of a received acoustic waveform representing a 31-bit hexadecimal value of 0x72361739, which includes a 7-bit Barker code (0x72; leading zero is omitted), a 16-bit payload, and an 8-bit cyclic redundancy check (CRC) code. Considering that the PZT is polarized in the direction of its wall thickness and vibrates radially, the acoustic signal is mainly radiated normal to the wall surface of the PZT over its entire circumference, as shown in the beam pattern [Fig. 4(c)]. The mean source level of the acoustic signal for the front 180° is 156.3 dB. This translates into a theoretical transmission range of up to 400 m in a quiet environment, equivalent to the range of a commercial injectable transmitter [10], which has routinely been demonstrated to possess detection ranges on the order of 150–200 m in the immediate forebay of a large hydroelectric dam. It is worth noting that the practical communication range is affected by a variety of environmental parameters, such as water depth, flow, temperature, salinity, and multipath in shallow water. Since the main body of the Lab-on-a-Fish (i.e., the PCB and microbattery) blocks the acoustic signals emitted from the back of the PZT, as with all existing commercial transmitters, the signal strength toward the rear of the tag is much weaker. The setup to obtain the source level has been detailed previously [10].

A communication protocol [Fig. 4(d)] for reliable and robust transmission of time-variant acoustic signals was developed, to overcome the challenges in underwater acoustic communication associated with high path loss, time-varying propagation, and Doppler spread along the channel [45]. The key to the successful concurrent communications of multiple fish is the unique "tag code" and the "pulse rate interval (PRI) filter." The protocol is based on the transmission of a pulse train of multiplexed messages. The interval between transmitted messages is referred to as the PRI [10]. The Lab-on-a-Fish transmits the 31-bit acoustic signals $i + 1$ times with PRI_1.

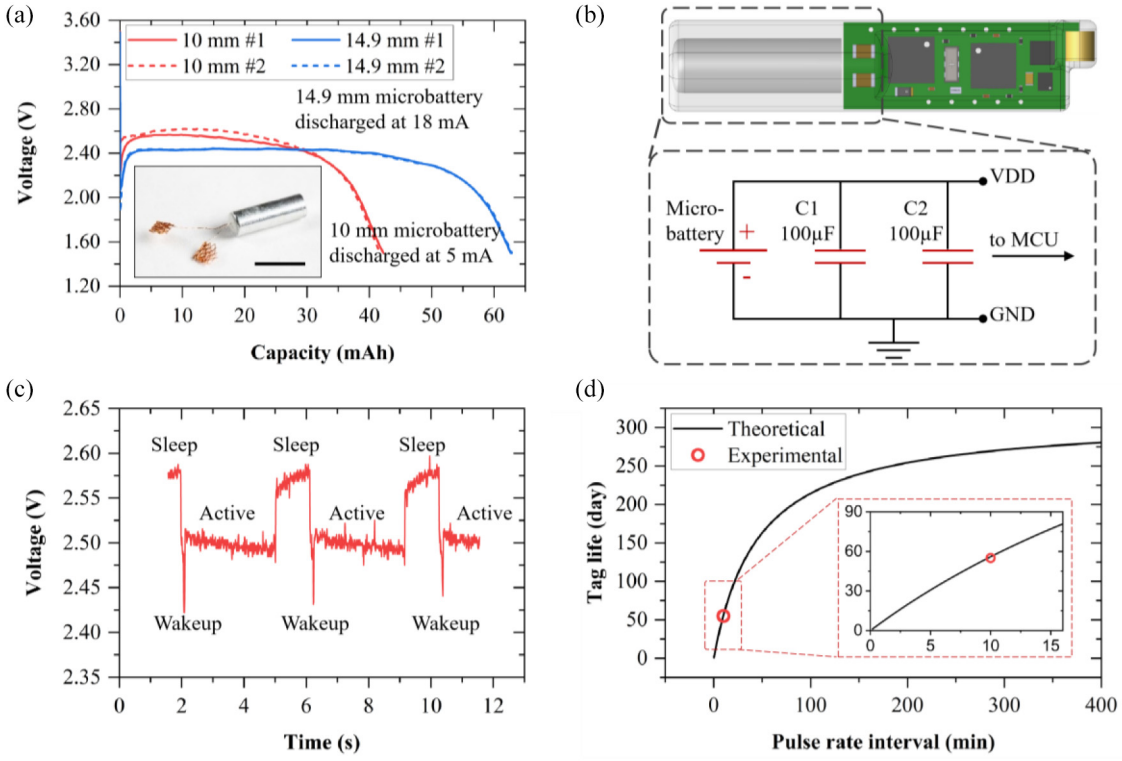

Fig. 5. Design and characterizations of the microbattery-enabled low-power system. (a) Discharge curves for the microbattery at high discharge currents of 18 and 5 mA for the 14.9- and 10-mm versions of the microbattery, respectively. The inset shows a photograph of the 14.9-mm microbattery. The scale bar is 10 mm. (b) Schematic of the power supply circuit. The microbattery is in parallel with two decoupling capacitors for a sustainable supply to the system. VDD is voltage drain drain and GND is ground. (c) Discharge curve for the integrated microbattery during regular operation of the Lab-on-a-Fish. (d) Device service life (tag life) as a function of pulse interval. The solid curve is the theoretical prediction and circles mark experimental results.

The first signal contains the unique identification code (tag code) of the Lab-on-a-Fish. The next i signals contain sensor data, where the first 2 bytes of the payload are a replica of the tag code, and the following 2 bytes are the actual sensor data. This bundle of $i + 1$ transmissions is repeated j times with PRI_2 to permit the receiver to decode the transmitted tag code along with its sensor data. Subsequently, PRI_3 is used to denote the interval between new measurements. On the receiving side, the decoder will trigger a "success" only if a pulse train of multiple transmissions with the predefined interval, and each with an identical starting "tag code" is received. When the information from an array of acoustic receivers is combined, the 3-D migrational trajectories of tagged animals can be constructed. The acoustic communication protocol was verified with three concurrent transmitting Lab-on-a-Fish, in a highly confined laboratory space that produces high scattering effects of the acoustic signal, highlighting the efficacy of the designed communication protocol.

3) Design and Characterizations of the Microbattery-Enabled Low-Power System: The methods to maximize the device longevity apply collective engineering efforts across improvements in battery chemistry, electronic circuit efficiency, and power-saving algorithms. A high-performance microbattery based on $\mathrm{Li/CF}_x$ chemistry was developed to power the Lab-on-a-Fish. Superior to traditional silver-oxide button-cell batteries commonly used in small commercial transmitters, our $\mathrm{Li/CF}_x$ batteries exhibit high volumetric energy density (528 $\mathrm{Wh{\cdot}L^{-1}}$), high average operating voltage (up to 3 V), and a wide operating temperature range (−5 °C to 25 °C) [46]. As demonstrated by the discharge profile shown in Fig. 5(a), the microbattery continuously supplies a voltage above 2 V, even at a high discharge current of 18 mA, for a total capacity of over 58 mAh. The jelly roll structured [47] microbattery features a cylindrical aluminum package (diameter: 4.7 mm, length: 14.9 mm), to be compatible with the Lab-on-a-Fish's cylindrical capsule body. Alternatively, an even smaller version of the microbattery with a length of 10 mm has been developed and can deliver a total capacity of more than 38 mAh.

A low-power system was achieved by combining hardware and software optimization techniques. To reduce the overall dynamic power, the MCU is programmed to run at its full operational speed of 10 MHz. This is because at higher frequencies, the fixed bias current becomes a negligible portion of the power consumption. To reduce the static power, the MCU was put in a retention sleep mode with all the sensors disconnected using an N-channel enhancement mode field-effect transistor. All the bidirectional input/output pins of the MCU were pulled to high or driven to low to prevent them from floating. At any point in the program, only the currently needed features were enabled.

The microbattery was connected in parallel with two decoupling capacitors to form the power supply [Fig. 5(b)]. The overall discharge curve of the integrated microbattery during the regular operation of the Lab-on-a-Fish (including data acquisition, onboard data processing, and acoustic wireless communication) is shown in Fig. 5(c). Despite a high inrush current (up to 20 mA) required to charge the capacitors

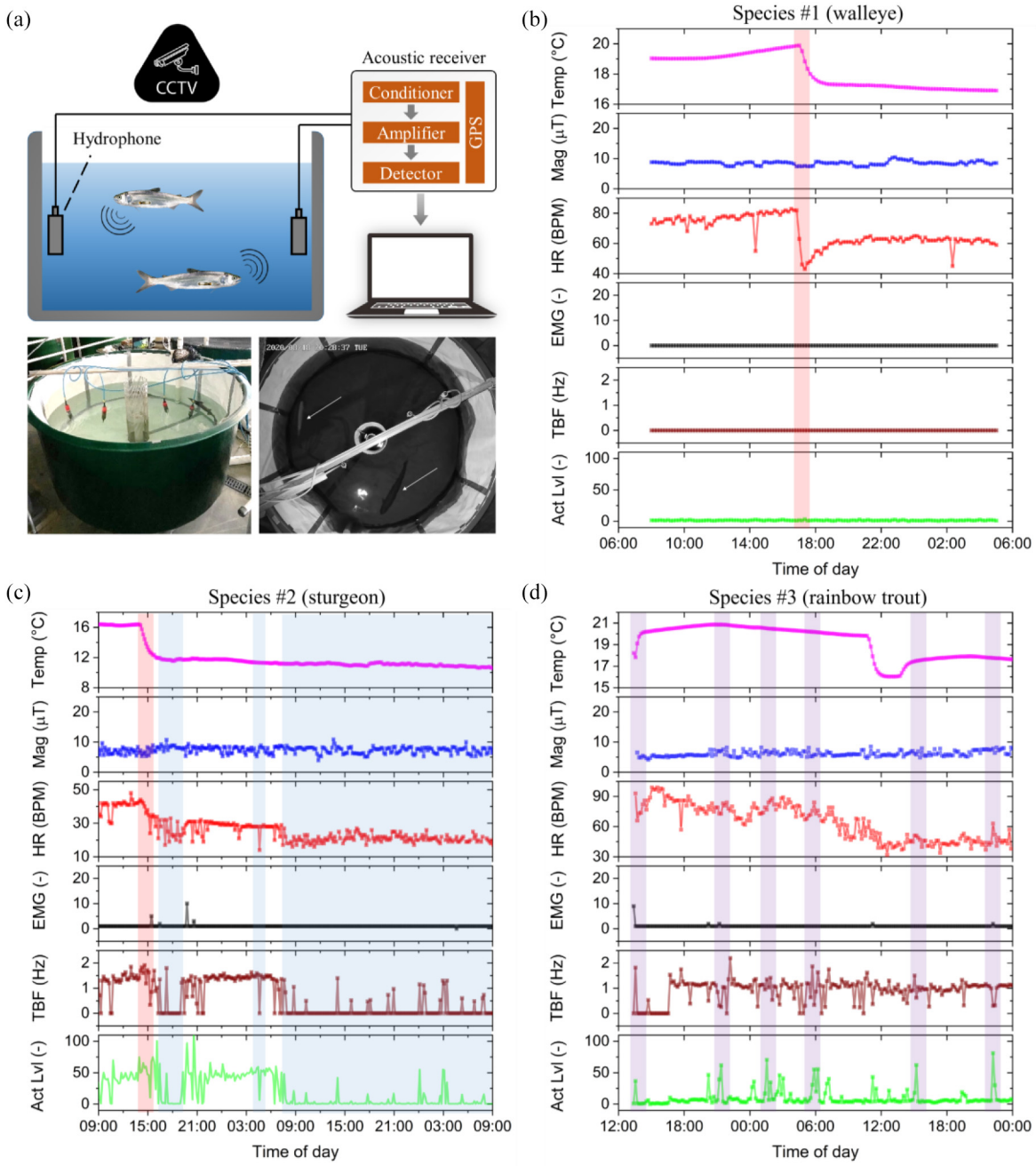

Fig. 6. *In vivo* system validation of the Lab-on-a-Fish during long-term monitoring of rainbow trout, walleye, and sturgeon. (a) Schematic illustration and photographs of the experimental setup, showing fish with surgically implanted Lab-on-a-Fish devices held in a tank, an array of hydrophones to acquire acoustic signals, an acoustic receiver system to detect the transmitted acoustic message, and a computer with software for real-time signal collection and interpretation. (b)–(d) Real-time temperature, magnetic field, HR, EMG index, TBF, and activity level data from walleye, sturgeon, and rainbow trout.

and inductors to turn on the system during system wake-up, there is only a relatively small instantaneous voltage drop of 0.15 V, owing to the low internal impedance of the microbattery. This small voltage drop ensures that sufficiently high voltage can be continuously supplied to the system, guaranteeing the system's normal operation. Various experiments were performed to measure energy consumption and to estimate the longevity of the Lab-on-a-Fish. The optimized current consumption of each module (Table S1 in the supplementary material) serves as the basis for calculating the system's total energy consumption and predicting the tag life. Theoretical predictions of tag life have been calculated and plotted with experimental results [Fig. 5(d)]. The longer the PRI (i.e., the less frequent the data acquisition and transmission occurs), the longer the tag life. The tag life can also be increased by reducing the number of active sensors, as each of the available sensors can be disabled depending on the user's need. The tag life is limited to 280 days because an 8-μA static current maintains the Lab-on-a-Fish's minimal functionalities (during device sleep). Further enhancement of the tag's lifetime could be achieved by: 1) increasing the capacity of the microbattery and 2) improving the onboard algorithm, e.g., the ECG/EMG algorithm, such that a comparable performance could be achieved with a shorter data sampling duration.

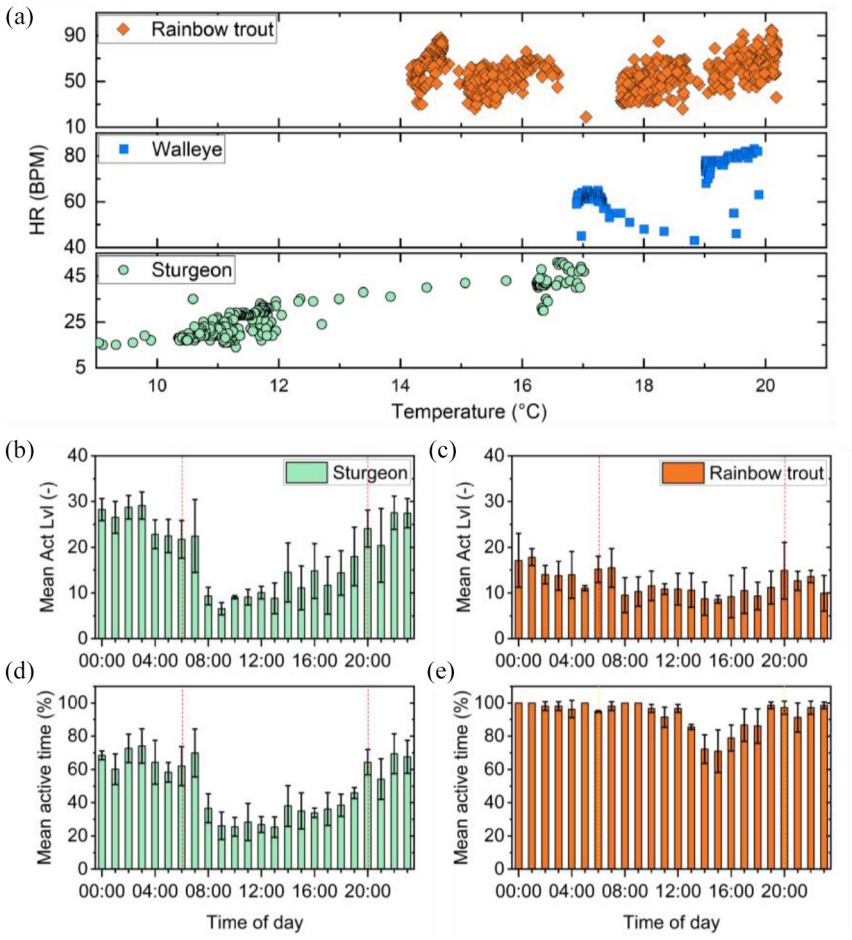

Fig. 7. Correlation of fish physiology with behavior and environmental stimulus. (a) Temperature dependence of HR for rainbow trout, walleye, and sturgeon. (b)–(e) Day–night pattern analysis. (b) Average activity level for sturgeon, and (c) rainbow trout. (d) Average active time for sturgeon, and (e) rainbow trout throughout the day. The statistics are based on a sample size of three for each species. The dashed lines represent the average times of sunrise and sunset for the experiments.

4) Demonstration of the Lab-on-a-Fish: The Lab-on-a-Fish was surgically implanted in ten subjects for long-term *in vivo* device validation. Three fish species—rainbow trout, walleye, and sturgeon—were adopted for the study. A schematic illustration and photograph of the experimental setup are shown in Fig. 6(a). After surgical implantation, the subjects were released in a temperature-controlled tank with a constant, flow-through water supply of filtered water from the Columbia River. Four hydrophones were set up in the tank for data acquisition, and were connected to a PC for real-time data interpretation. An infrared video recorder with night vision was installed above the tank for confirming fish behavior and correlating it with sensor data.

Fig. 6(b) shows *in vivo,* real-time temperature, magnetic field, HR, EMG index, TBF, and activity level (Act Lvl) data for free-swimming walleye. The HR of the tagged walleye shows a strong response to the ambient temperature change. As shown on the left-hand side of Fig. 6(b), a gradual increase in ambient temperature (resulting from the natural temperature increase of the water) is accompanied by a gradual increase in the walleye's HR. The ambient temperature variance at around 5 P.M. was introduced intentionally by manually adjusting the ratio of cold and warm water to investigate the behavior and physiology response to environmental stimulus. When the tagged walleye experienced a temperature drop of 3 °C (from 20 °C to 17 °C, as highlighted by the red region), the walleye's HR dropped drastically from 86 to 46 BPM. After reaching the minimum HR, even though the temperature continues to fall, the HR rebounds and stabilizes to around 60 BPM, suggesting that the walleye acclimated to the environmental change. Simultaneous TBF, EMG, and activity level data all remained low, further indicating that the cardiac change was primarily caused by the ambient temperature change.

The response of HR to ambient temperature was also confirmed in the tagged sturgeon. As highlighted by the red region in Fig. 6(c), the temperature drop from 16 °C to 12 °C at 3 P.M. coincides with the decrease in HR of white sturgeon from 44 to 32 BPM. Nevertheless, sturgeon shows a slower thermal response, indicated by the gradual decrease of HR compared to the drastic change observed in walleye.

Furthermore, behavior-induced physiology variance was observed in the sturgeon. Unlike the stable HR seen in the walleye, the sturgeon displays unstable HR with a large variation. This can be correlated with the swimming activity, as evident by the TBF and activity level (Act Lvl) measurements. Decreased swimming activity also coincided with lower HR, as highlighted by the blue regions.

Behavior-dependent physiology was also confirmed in the rainbow trout. As highlighted in the purple regions in Fig. 6(d), the peaks observed in the activity level correspond with the peaks found in HR measurements, showing a positive relationship between activity level and HR. Thermal response in rainbow trout was observed to be less significant than that in other species of fish.

A low output of EMG measurements (as opposed to the motion sensor) of fish behavior was found for all three species. This lack of performance and reliability has been identified by others and is likely a result of the requirement for relatively precise probe placement, the distance between probes, and debate over which specific muscle is responsible for the activities [48]. EMG electrodes are usually only implanted into either red or white muscle tissue and therefore, fail to monitor all movements of the subject [49]. The EMG of pectoral fin muscles in swimming sturgeons apparently indicates an almost complete absence of muscle activity [50].

Plotting ambient temperature against the HR shows an apparent correlation between environmental temperature and cardiac output for each species [Fig. 7(a)]. Sturgeons showed a pronounced diel pattern with a large difference in time spent swimming and activity level between day and night, while rainbow trout remained active throughout most of the day, but at a lower activity level. Based on the small sample size ($N = 3$), sturgeon spent significantly less time swimming during the day ($38 \pm 13\%$) from 6 A.M. (sunrise) to 8 P.M. (sunset) than at night ($65 \pm 6\%$). The diel pattern of the sturgeon activity level was also confirmed: $13 \pm 5\%$ for the day and $26 \pm 3\%$ at night. A mild diel pattern was observed in rainbow trout, with the portions of time spent swimming being $90 \pm 10\%$ (day), $98 \pm 2\%$ (night), and the activity levels being 11 ± 2 (day) and 14 ± 2 (night). These findings on the behavioral patterns of rainbow trout and white sturgeon agreed with previous work [51], [52]. Behavior data for each individual fish are detailed in Fig. S7 in the supplementary material.

Implantation into a rainbow trout, walleye, and sturgeon for up to four weeks showed minimal foreign-body reaction (Fig. S8 in the supplementary material) and did not cause severe negative effects on natural behavior of the fish, indicating the suitability of the Lab-on-a-Fish for long-term *in vivo* studies.

III. Conclusion

A miniaturized, fully integrated, wireless biotelemetry tag has been developed, manufactured, and validated through *in vivo* fish experiments in captivity. Lab-on-a-Fish surpasses current biotelemetry tags, which fail to offer desired levels of functionality, convenience, reliability, or accuracy while minimizing effects on the fish. Lab-on-a-Fish integrates temperature, pressure, triaxial acceleration, triaxial gyration, triaxial magnetic field, ECG, and EMG sensors with intelligent onboard data processing algorithms in a single miniaturized platform. Measurement data are collected and processed onboard in real time, stored, and transmitted through wireless acoustic communication. Excellent microbattery performance combined with the low-power system design extends the tag's service life to support consistency, repeatability, and robustness. The scalable manufacturing scheme facilitates potential scaled deployment and offers immediate opportunities for broad distribution in the fishery and marine biology communities. Three physiologically distinct fish species—rainbow trout, walleye, and sturgeon—were adopted for the study to validate the effectiveness of the developed Lab-on-a-Fish for a wide variety of species. *In vivo*, real-time physiology, behavior, and environmental monitoring capabilities of the Lab-on-a-Fish quantify the ambient conditions, physiology, and activity patterns, and allow correlation of physiological response with environmental stimulus or cumulated behavior. The combination of these features paves the way for ecologists to continuously monitor most aspects of an aquatic animal's behavior and physiology (e.g., location, locomotion, caloric expenditure, predation). It also enables the use of animals as sensors of the environment (e.g., temperature, magnetic field, and depth). Lab-on-a-fish may deliver information on the *in situ* physiology, behavior, and ecology of wild aquatic animals at challenging locations where device limitations have previously restricted tests to model organisms in controlled settings.

Acknowledgment

This work was conducted at Pacific Northwest National Laboratory (PNNL), which is operated by Battelle for DOE under Contract DE-AC05-76RL01830. Fish care and use for the study were approved by Pacific Northwest National Laboratory's Institutional Animal Care and Use Committee (protocol No. 2019-02) following the 8th Edition Guide for the Care and Use of Laboratory Animals (NRC 2011). The authors acknowledge M. Myjak and R. Lundy for the PCB layout, A. Dao for the ECG algorithm, and R. Elsinghorst and A. Salalila for the manufacturing.

References

[1] N. E. Hussey *et al.*, "Aquatic animal telemetry: A panoramic window into the underwater world," *Science*, vol. 348, no. 6240, Jun. 2015, Art. no. 1255642.

[2] C. Laplanche, T. A. Marques, and L. Thomas, "Tracking marine mammals in 3D using electronic tag data," *Methods Ecol. Evol.*, vol. 6, no. 9, pp. 987–996, Sep. 2015.

[3] R. Kays, M. C. Crofoot, W. Jetz, and M. Wikelski, "Terrestrial animal tracking as an eye on life and planet," *Science*, vol. 348, no. 6240, p. aaa2478, Jun. 2015.

[4] S. K. Lowerre-Barbieri, R. Kays, J. T. Thorson, and M. Wikelski, "The ocean's movescape: Fisheries management in the bio-logging decade (2018–2028)," *ICES J. Marine Sci.*, vol. 76, no. 2, pp. 477–488, Mar./Apr. 2019.

[5] D. March, L. Boehme, J. Tintoré, P. J. Vélez-Belchi, and B. J. Godley, "Towards the integration of animal-borne instruments into global ocean observing systems," *Global Change Biol.*, vol. 26, no. 2, pp. 586–596, Feb. 2020.

[6] B. A. Block *et al.*, "Tracking apex marine predator movements in a dynamic ocean," *Nature*, vol. 475, no. 7354, pp. 86–90, Jun. 2011.

[7] B. A. Block *et al.*, "Electronic tagging and population structure of Atlantic bluefin tuna," *Nature*, vol. 434, no. 7037, pp. 1121–1127, Apr. 2005.

[8] S. T. Kessel *et al.*, "Predictable temperature-regulated residency, movement and migration in a large, highly mobile marine predator (negaprion brevirostris)," *Marine Ecol. Progr. Ser.*, vol. 514, pp. 175–190, Nov. 2014.

[9] R. Mueller, S. Liss, and Z. D. Deng, "Implantation of a new micro acoustic tag in juvenile Pacific Lamprey and American Eel," *J. Vis. Exp.*, no. 145, Mar. 2019, Art. no. e59274.

[10] Z. D. Deng *et al.*, "An injectable acoustic transmitter for juvenile salmon," *Sci. Rep.*, vol. 5, no. 1, pp. 1–6, 2015.

[11] J. Lu *et al.*, "A small long-life acoustic transmitter for studying the behavior of aquatic animals," *Rev. Sci. Instrum.*, vol. 87, no. 11, Nov. 2016, Art. no. 114902.

[12] R. Harcourt *et al.*, "Animal-borne telemetry: An integral component of the ocean observing toolkit," *Front. Marine Sci.*, vol. 6, p. 326, Jun. 2019.

[13] M. R. Donaldson, S. G. Hinch, C. D. Suski, A. T. Fisk, M. R. Heupel, and S. J. Cooke, "Making connections in aquatic ecosystems with acoustic telemetry monitoring," *Front. Ecol. Environ.*, vol. 12, no. 10, pp. 565–573, Dec. 2014.

[14] A.-L. Harrison *et al.*, "The political biogeography of migratory marine predators," *Nat. Ecol. Evol.*, vol. 2, no. 10, pp. 1571–1578, Oct. 2018.

[15] J. D. Metcalfe and G. P. Arnold, "Tracking fish with electronic tags," *Nature*, vol. 387, no. 6634, pp. 665–666, Jun. 1997.

[16] C. C. Wilmers, B. Nickel, C. M. Bryce, J. A. Smith, R. E. Wheat, and V. Yovovich, "The golden age of bio-logging: How animal-borne sensors are advancing the frontiers of ecology," *Ecology*, vol. 96, no. 7, pp. 1741–1753, Jul. 2015.

[17] D. J. Madigan *et al.*, "Assessing niche width of endothermic fish from genes to ecosystem," *Proc. Nat. Acad. Sci.*, vol. 112, no. 27, pp. 8350–8355, Jul. 2015.

[18] R. E. Whitlock *et al.*, "Direct quantification of energy intake in an apex marine predator suggests physiology is a key driver of migrations," *Sci. Adv.*, vol. 1, no. 8, Sep. 2015, Art. no. e1400270.

[19] N. Queiroz *et al.*, "Global spatial risk assessment of sharks under the footprint of fisheries," *Nature*, vol. 572, no. 7770, pp. 461–466, Aug. 2019.

[20] Y. Yang, "Multi-tier computing networks for intelligent IoT," *Nat. Electron.*, vol. 2, no. 1, pp. 4–5, Jan. 2019.

[21] Q. Guan, F. Ji, Y. Liu, H. Yu, and W. Chen, "Distance-vector-based opportunistic routing for underwater acoustic sensor networks," *IEEE Internet Things J.*, vol. 6, no. 2, pp. 3831–3839, Apr. 2019.

[22] F. Broell, C. Burnell, and C. T. Taggart, "Measuring abnormal movements in free-swimming fish with accelerometers: Implications for quantifying tag and parasite load," *J. Exp. Biol.*, vol. 219, no. 5, pp. 695–705, Mar. 2016.

[23] R. S. Brown, R. A. Harnish, K. M. Carter, J. W. Boyd, K. A. Deters, and M. B. Eppard, "An evaluation of the maximum tag burden for implantation of acoustic transmitters in juvenile chinook salmon," *North Amer. J. Fish. Manag.*, vol. 30, no. 2, pp. 499–505, Apr. 2010.

[24] H. Dewar, M. Deffenbaugh, G. Thurmond, K. Lashkari, and B. A. Block, "Development of an acoustic telemetry tag for monitoring electromyograms in free-swimming fish," *J. Exp. Biol.*, vol. 202, no. 19, pp. 2693–2699, Oct. 1999.

[25] G. Premsankar, M. Di Francesco, and T. Taleb, "Edge computing for the Internet of Things: A case study," *IEEE Internet Things J.*, vol. 5, no. 2, pp. 1275–1284, Apr. 2018.

[26] Y. Yang, K. Xu, T. Vervust, and J. Vanfleteren, "Multifunctional and miniaturized flexible sensor patch: Design and application for *in situ* monitoring of epoxy polymerization," *Sens. Actuat. B, Chem.*, vol. 261, pp. 144–152, May 2018.

[27] J. Xiao *et al.*, "Understanding and applying coulombic efficiency in lithium metal batteries," *Nat. Energy*, vol. 5, no. 8, pp. 561–568, Aug. 2020.

[28] Y. Wang *et al.*, "Fundamental understanding and rational design of high energy structural microbatteries," *Nano Energy*, vol. 43, pp. 310–316, Jan. 2018.

[29] H. Li, Z. D. Deng, Y. Yuan, and T. J. Carlson, "Design parameters of a miniaturized piezoelectric underwater acoustic transmitter," *Sensors*, vol. 12, no. 7, pp. 9098–9109, 2012.

[30] Y. Yang and Z. D. Deng, "Stretchable sensors for environmental monitoring," *Appl. Phys. Rev.*, vol. 6, no. 1, 2019, Art. no. 011309.

[31] H. Chen *et al.*, "Micro-battery development for juvenile salmon acoustic telemetry system applications," *Sci. Rep.*, vol. 4, p. 3790, Jan. 2014.

[32] T. Dodson, T. M. Grothues, J. H. Eiler, J. A. Dobarro, and R. Shome, "Acoustic-telemetry payload control of an autonomous underwater vehicle for mapping tagged fish," *Limnol. Oceanogr. Methods*, vol. 16, no. 11, pp. 760–772, Nov. 2018.

[33] P. Boyd *et al.*, "A temperature-monitoring vaginal ring for measuring adherence," *PLoS One*, vol. 10, no. 5, 2015, Art. no. e0125682.

[34] M. Dudek *et al.*, "A comparison of the anorectic effect and safety of the alpha2-adrenoceptor ligands guanfacine and yohimbine in rats with diet-induced obesity," *PLoS One*, vol. 10, no. 10, 2015, Art. no. e0141327.

[35] N. Yoshida, H. Mitamura, H. Okamoto, and N. Arai, "Measurement of activity for sit-and-wait predator, red-spotted grouper, using acoustic acceleration transmitter," *J. Adv. Marine Sci. Technol. Soc.*, vol. 21, no. 1, pp. 1–5, 2015.

[36] Y. Yang *et al.*, "Facile fabrication of stretchable Ag nanowire/polyurethane electrodes using high intensity pulsed light," *Nano Res.*, vol. 9, no. 2, pp. 401–414, 2016.

[37] Y. Yang *et al.*, "3D multifunctional composites based on large-area stretchable circuit with thermoforming technology," *Adv. Electron. Mater.*, vol. 4, no. 8, 2018, Art. no. 1800071.

[38] Y. Yang *et al.*, "Design and fabrication of a flexible dielectric sensor system for *insitu* and real-time production monitoring of glass fibre reinforced composites," *Sens. Actuat. A, Phys.*, vol. 243, pp. 103–110, Jun. 2016.

[39] Y. Yang *et al.*, "Design and integration of flexible sensor matrix for *insitu* monitoring of polymer composites," *ACS Sens.*, vol. 3, no. 9, pp. 1698–1705, 2018.

[40] Y. Yang *et al.*, "Fully integrated flexible dielectric monitoring sensor system for real-time *insitu* prediction of the degree of cure and glass transition temperature of an epoxy resin," *IEEE Trans. Instrum. Meas.*, vol. 70, pp. 1–9, 2021. [Online]. Available: https://ieeexplore.ieee.org/abstract/document/9359661?casa_token=rwv8-5yn4rEAAAAA:uowSBSrbDV0C59r0v7vxjsYVwb-8rXvkMhdCI1hZbf78rKUEpY3Bnwwvo-TIkex9zELAc9hnzCg

[41] K. Norland *et al.*, "Sequence variants with large effects on cardiac electrophysiology and disease," *Nat. Commun.*, vol. 10, no. 1, p. 4803, Oct. 2019.

[42] J. Pan and W. J. Tompkins, "A real-time QRS detection algorithm," *IEEE Trans. Biomed. Eng.*, vol. BME-32, no. 3, pp. 230–236, Mar. 1985.

[43] R. Kawabe, T. Kawano, N. Nakano, N. Yamashita, T. Hiraishi, and Y. Naito, "Simultaneous measurement of swimming speed and tail beat activity of free-swimming rainbow trout *Oncorhynchus mykiss* using an acceleration data-logger," *Fish. Sci.*, vol. 69, no. 5, pp. 959–965, Oct. 2003.

[44] D. B. Kilfoyle and A. B. Baggeroer, "The state of the art in underwater acoustic telemetry," *IEEE J. Ocean. Eng.*, vol. 25, no. 1, pp. 4–27, Jan. 2000.

[45] A. Song, M. Stojanovic, and M. Chitre, "Editorial underwater acoustic communications: Where we stand and what is next?" *IEEE J. Ocean. Eng.*, vol. 44, no. 1, pp. 1–6, Jan. 2019.

[46] Y. Wang *et al.*, "Lithium and lithium ion batteries for applications in microelectronic devices: A review," *J. Power Sources*, vol. 286, pp. 330–345, Jul. 2015.

[47] B. Wu *et al.*, "Good practices for rechargeable lithium metal batteries," *J. Electrochem. Soc.*, vol. 166, no. 16, p. A4141, 2019.

[48] J. D. Metcalfe, S. Wright, C. Tudorache, and R. P. Wilson, "Recent advances in telemetry for estimating the energy metabolism of wild fishes," *J. Fish Biol.*, vol. 88, no. 1, pp. 284–297, Jan. 2016.

[49] A. C. Gleiss, J. J. Dale, K. N. Holland, and R. P. Wilson, "Accelerating estimates of activity-specific metabolic rate in fishes: Testing the applicability of acceleration data-loggers," *J. Exp. Marine Biol. Ecol.*, vol. 385, nos. 1–2, pp. 85–91, Apr. 2010.

[50] C. D. Wilga and G. V. Lauder, "Locomotion in sturgeon: Function of the pectoral fins," *J. Exp. Biol.*, vol. 202, no. 18, pp. 2413–2432, 1999.

[51] M. J. Parsley, N. D. Popoff, C. D. Wright, and B. K. van der Leeuw, "Seasonal and diel movements of white sturgeon in the lower Columbia River," *Trans. Amer. Fish. Soc.*, vol. 137, no. 4, pp. 1007–1017, Jul. 2008.

[52] S. J. Cooke, K. P. Chandroo, T. A. Beddow, R. D. Moccia, and R. S. McKinley, "Swimming activity and energetic expenditure of captive rainbow trout *Oncorhynchus mykiss* (Walbaum) estimated by electromyogram telemetry," *Aquacult. Res.*, vol. 31, no. 6, pp. 495–505, Jun. 2000.

Yang Yang (Member, IEEE) received the Ph.D. degree in electrical engineering from IMEC and Ghent University, Ghent, Belgium, in 2017.

From 2017 to 2018, he was a Postdoctoral Fellow with Japan Society for the Promotion of Science, Osaka University, Suita, Japan. From 2018 to 2020, he was a Post Doctorate Research Associate and then a Staff Member with Pacific Northwest National Laboratory, Richland, WA, USA. In 2020, he joined the Institute of Deep-Sea Science and Engineering, Chinese Academy of Sciences, Chinese Academy of Sciences, Sanya, China, as an Associate Professor. He has authored or coauthored over 30 peer-reviewed papers and conference proceedings. His current research interests include flexible and stretchable sensor systems and marine electronics.

Jun Lu (Member, IEEE) received the Ph.D. degree from the Department of Electrical and Computer Engineering, State University of New York, Binghamton, NY, USA, in 2012.

He is currently Senior Electrical Engineer with the Pacific Northwest National Laboratory, Richland, WA, USA. His research interests include autonomous sensors for environmental assessment, and low-power electronics design for tracking and sensing technologies.

Brett D. Pflugrath, photograph and biography not available at the time of publication.

Huidong Li received the bachelor's degree in chemical engineering from Tsinghua University, Beijing, China, in 2000, and the Ph.D. degree in materials science and engineering from Drexel University, Philadelphia, PA, USA, in 2008.

He is currently a Senior Materials Scientist and the Team Lead of the Sensing, Measurement and Forecasting Team, Earth Systems Science Division, Pacific Northwest National Laboratory, Richland, WA, USA. He has published more than 20 peer-reviewed articles and is a co-inventor of ten patents. His research interests include underwater acoustic telemetry, piezoelectric materials and devices, energy harvesting, and environmental sensing.

Jayson J. Martinez received the bachelor's and master's degrees in mechanical engineering from Portland State University, Portland, OR, USA, in 2008 and 2009, respectively.

He has been a Research Engineer with the Energy and Environment Directorate, Pacific Northwest National Laboratory (PNNL), Richland, WA, USA, since December 2009. He is the Technical Manager of the PNNL Bio-Acoustics and Flow Laboratory which is accredited by The American Association for Laboratory Accreditation. He has coauthored 30 journal articles and 38 technical reports. He has contributed to the research and design of different systems that address engineering and ecological concerns related to hydro, wind, marine, and hydrokinetic energy systems. In addition to research and design, he has been involved extensively with the field deployment of these technologies as well as the data reduction and analysis of the data gathered in the field.

Siddhartha Regmi, photograph and biography not available at the time of publication.

Bingbin Wu, photograph and biography not available at the time of publication.

Jie Xiao, photograph and biography not available at the time of publication.

Zhiqun Daniel Deng received the Ph.D. degree from the University of Illinois at Urbana-Champaign, Champaign, IL, USA, in 2003.

He is a Laboratory Fellow with the Pacific Northwest National Laboratory, Richland, WA, USA, and an Adjunct Professor of Mechanical Engineering with Virginia Tech, Blacksburg, VA, USA. He directs the Bio-Acoustics and Flow Laboratory, an accredited multidisciplinary Research and Development laboratory, addressing a broad range of engineering and ecological issues, with an emphasis on environmental monitoring and risk assessment for hydropower, wind, marine, and hydrokinetic energy systems. He has authored or coauthored over 130 journal articles. His research interests include integrated sensor system, energy harvesting, and renewable energy.